buildings

MDPI

Article

Effect of Nano-Clay Dispersion on Pore Structure and Distribution of Hardened Cement Paste

Hongjuan Wu [1], Chengqin Chen [1,*], Wei Zhang [1], Rui Wang [1] and Wengang Zhang [2]

[1] School of Civil Engineering, Northwest Minzu University, Lanzhou 730000, China; wuhjnmu@163.com (H.W.); zhangwnmu@126.com (W.Z.); wruizz1900@yeah.net (R.W.)
[2] School of Civil Engineering and Geomatics, Shandong University of Technology, Zibo 255049, China; ziwuzizwg@sdut.edu.cn
* Correspondence: cccnmu@126.com

Abstract: Nano-clay has the potential to improve the properties of cement-based materials. However, the effectiveness of this improvement is influenced by the dispersion of the nano-clay. The effects of different nano-clay dispersion techniques on cement-based material properties and pore structure complexity were studied. The samples were prepared using manual and mechanical dispersion methods. The mechanical properties of the specimens were evaluated, and the pore characteristics of the cement-based materials were analysed using mercury intrusion porosimetry. The study investigated the effect of the dispersion method on the nano-clay dispersion. The complexity of the pore structure was evaluated using a fractal model, and the relationship between the fractal dimension, mechanical properties, and pore structure was analysed. The findings indicate that mechanical dispersion results in better dispersion than manual dispersion, and the mechanical properties of mechanical dispersion are superior to those of manual dispersion. Nano-clay particles can improve the internal pore structure of cement materials. Through mathematical calculation, the surface fractal dimension is between 2.90 and 2.95, with good fractal characteristics. There is a good correlation between the surface fractal dimension and the mechanical properties. The addition of nano-clay can reduce the complexity of the pore structure, and the fractal dimension has an excellent linear relationship with the pore structure.

Keywords: nano-clay; dispersivity; pore structure; fractal dimension; mechanical properties

Citation: Wu, H.; Chen, C.; Zhang, W.; Wang, R.; Zhang, W. Effect of Nano-Clay Dispersion on Pore Structure and Distribution of Hardened Cement Paste. *Buildings* **2023**, *13*, 2753. https://doi.org/10.3390/buildings13112753

Academic Editors: A. B. M. Saiful Islam and Akter Hosen

Received: 5 October 2023
Revised: 25 October 2023
Accepted: 30 October 2023
Published: 31 October 2023

1. Introduction

Economic development has led to the construction of many structures in the marine environment, mainly using concrete. Nevertheless, the durability of concrete structures in harsh marine environments is becoming an increasingly severe problem. Concrete is typically subject to environmental factors, loads, and their associated effects during service. Such effects include corrosion of the reinforcement initiated by the infiltration of chloride ions, which can harm the durability and performance of the concrete. As a porous material, concrete's permeability is a crucial determinant of its durability and is determined by its pore structure [1–3]. Improving concrete durability is crucial in ensuring infrastructure serviceability in the long term [4]. In contrast to conventional mineral admixtures, nanomaterials comprise smaller particles, which can fill the pores and decrease porosity to enhance concrete durability. In recent years, nano-clay materials have become a popular research area of great interest in the civil engineering and construction industries. The development of nanomaterials has improved the performance and durability of existing materials and has driven the development of concrete materials toward multifunctionality and high performance. Many studies have been conducted on nanomaterials in concrete.

Studies have shown that nanomaterials can significantly improve the properties of cement-based materials [5–11]. Mohamed's [11] study found that nano-clay accelerates cement hydration, makes the microstructure dense, and improves its compressive strength.

Shoukry [12] et al. found that incorporating nano-kaolinite into cement mortar significantly increased its compressive and flexural strength. Including 3% nano-kaolinite resulted in a 24% increase in the compressive strength of cement specimens [13]. Langaroudi et al. [14] substituted cement with 1%, 2%, and 3% nano-clay and discovered that the cement-based materials' mechanical properties improved as the nano-clay concentration increased over 90 days. Moreover, nono-clay reduces the permeability, thereby improving the material's durability. Hong et al. [15] found similar conclusions when studying the permeability of cement-based materials. Nano-clay instead of cement can reduce permeability, attributed to the fact that nano-clay particles can not only fill pores but also promote cement hydration to improve the pore structure. In addition, it has been shown that the addition of nano-kaolinite fills the larger pores of the cement and refines the pores [16]. The pozzolanic reaction of the nano-clay during hydration produces additional C-S-H gel to fill the pores [14]. Nano-clay particles can serve as nucleation sites for the growth of C-S-H gels during cement hydration, thereby promoting cement hydration, filling pores, and creating a more uniform and dense concrete structure [17]. These effects can enhance cementitious materials' mechanical properties and microstructure by boosting the formation of C-S-H gels and decreasing $Ca(OH)_2$ to densify the cement. Zhang et al. [18] researched the impact of nano-kaolinite on the resistance of reinforced concrete to corrosion. The results indicate that incorporating nano-kaolinite increases the concrete's density, reduces the corrosion rate of steel bars, and enhances the material's resistance to corrosion. In summary, nano-clay materials can improve the pore structure of cement-based materials, thereby increasing their durability. However, due to the large specific surface area of nanomaterials, van der Waals forces can cause agglomeration and affect the dispersion of nanomaterials [19]. The dispersion technique of the nano-clay has been found to impact its dispersion and the hydration and mechanical properties of cement-based materials [20,21]. Therefore, it is necessary to study the effect of nano-clay dispersion on concrete properties.

In order to understand the pore structure of nano-clay cement specimens, it is necessary to analyse the pore structure of cement specimens. Generally, scanning electron microscopy (SEM) image analysis, gas adsorption, nuclear magnetic resonance (NMR), mercury intrusion porosimetry (MIP), and other methods are used. However, there are pores with different pore diameters in concrete, namely bubbles, capillary pores, gel pores, and small cracks caused by drying shrinkage, which lead to the random disorder and diversity of pore morphology and spatial distribution and make the microstructure of cement composites extremely chaotic and complex. These factors lead to conventional parameters such as porosity, pore diameter distribution, and pore surface area, being unable to accurately represent the complexity of the internal pores of concrete. According to fractal theory, the pores of porous materials have distinct fractal characteristics in terms of pore volume, surface area, and pore diameter distribution [22]. Recent fractal geometry studies have quantitatively analysed the pore structure of complex cement-based materials [23]. Applying fractal theory to concrete pore structures gives us new ideas and tools for studying pore structures. The fractal dimension of pores obtained from mathematical calculations can more accurately describe the distribution of concrete pore structures. The fractal dimension has unique advantages in revealing the discontinuities and irregularities of the pore structure [24] and can describe the complexity of the pore morphology and spatial distribution. Zarnaghi et al. [25] found that the fractal dimension is a parameter that can reflect the pore diameter distribution. Choi et al. [26] used the surface fractal dimension to characterise the microstructural changes in geopolymer composites at elevated temperatures. Yang et al. [27] analysed the pore structure in cement composites doped with ground slag and found that the surface fractal dimension reflects its complexity. Jin et al. [28] used a thermodynamically based fractal dimensional fractal model of pore surface area to determine its ability to quantitatively and accurately reflect the pore structure's complexity when studying concrete's freeze–thaw properties. Fractal theory has been used extensively in concrete materials, e.g., the surface fractal dimension of concrete materials [23,26–29] correlates with permeability and compressive strength. In addition, the surface fractal

dimension [30] is also closely related to various properties of the pore structure. Therefore, it is valid to use fractal theory to analyse and evaluate the complexity of the pore structure of concrete. However, there is a considerable variation in the current research on fractal dimensions due to differences in the understanding of fractal dimensions by different researchers and experimental conditions.

To understand the influence of nano-clay dispersion on the pore structure of cement-based materials and the impact of nano-clay on the complexity of the pore structure, this article studies the effects of dispersion methods and dosage on the dispersibility of nano-clay, conducts mechanical performance tests, observes the microstructure using scanning electron microscopy, and studies the pore structure of cement using mercury intrusion porosimetry. Fractal models are used to characterise the complexity of the pore structure. It is helpful further to understand the action mechanism of nano-clay in cement-based materials.

2. Materials and Methods

2.1. Raw Materials

Materials

The cement used in this study was P•O42.5R ordinary Portland cement; its chemical composition is detailed in Table 1. The test mixing water was tap water. The nano-clay material chosen for this paper was nano-kaolinite, which is refined by crushing raw kaolinite ore with a crusher, then using an impact mill for 40 min of ultra-fine grinding [31], and then calcining it. Its physical index, chemical composition, and activity index are detailed in Tables 2–4. The cement and nano-kaolinite characteristics are shown in Figure 1.

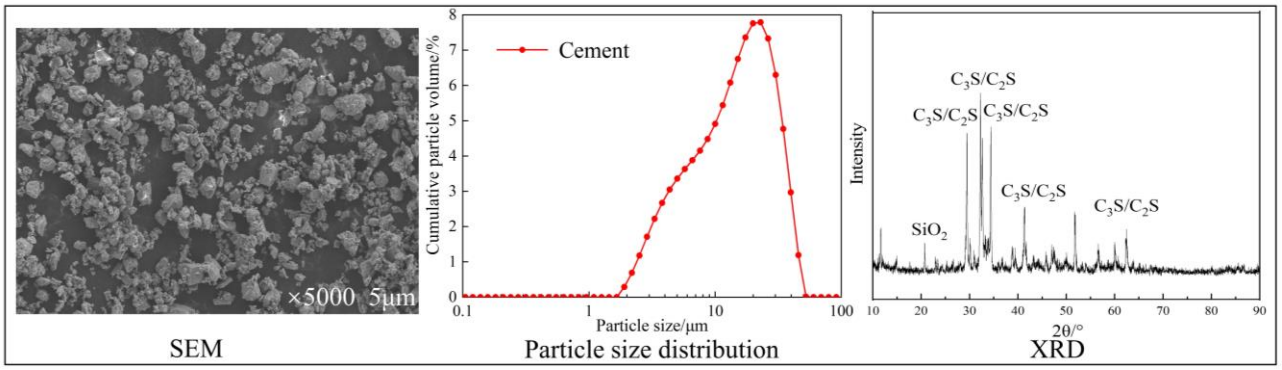

(**a**) Cement

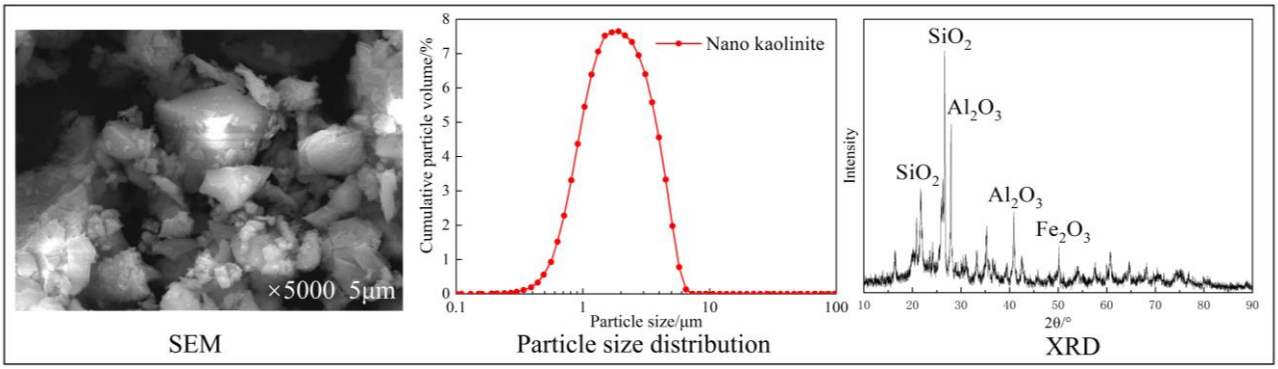

(**b**) Nano-kaolinite

Figure 1. Characteristics of cement and nano-kaolinite.

Table 1. Chemical composition of cement.

Sample	CaO	SiO_2	Al_2O_3	Fe_2O_3	MgO	SO_3
Content (%)	59.31	21.90	6.26	3.79	1.63	2.41

Table 2. Physical index of the nano-kaolinite clay.

Average Flake Diameter (nm)	Average Flake Thickness (nm)	Specific Surface Area (m^2/g)	Density (g/cm^3)
300–500	20–50	30	0.6

Table 3. Chemical composition of nano-kaolinite.

Sample	SiO_2	CaO	Al_2O_3	Fe_2O_3	MgO	K_2O	TiO_2	Na_2O
Content (%)	47.80	0.28	41.80	0.30	0.03	0.58	0.02	0.06

Table 4. Activity index of nano-kaolinite.

Time	3 Days	7 Days	28 Days
Activity index (%)	118	121	115

2.2. Mix Proportion and Specimens Preparation

An experimental study was carried out to investigate the effect of the dispersion method on the dispersibility. Dispersion of nano-kaolinite at different dosing levels of 0%, 0.75%, 1.0%, and 1.5% was carried out using manual and mechanical dispersion. The specimen numbers are shown in Table 5.

Table 5. Cement specimen numbers for different dispersion methods.

Sample	W (Nano-Clay) (%)	Disperse Method	Disperse Time (min)
NC0	0	-	-
NCH1	0.75	Hand	3
NCH2	1.00	Hand	3
NCH3	1.50	Hand	3
NCM1	0.75	Machine	3
NCM2	1.00	Machine	3
NCM3	1.50	Machine	3

The nano-kaolinite was mixed with water and stirred for 3 min using both manual dispersion and mechanical dispersion to make nano-kaolinite suspensions, which were stirred with cement according to the water–cement ratio of 0.5 to make cement paste. This was then poured into the test mould to make a prismatic cylinder of 40 mm × 40 mm × 160 mm, and then, after being removed from the mould, it was placed into a standard maintenance box to maintain it to the specified age for 24 h at a standard temperature of 20 ± 1 °C and relative humidity of ≥95%. The specimen preparation process is shown in Figure 2.

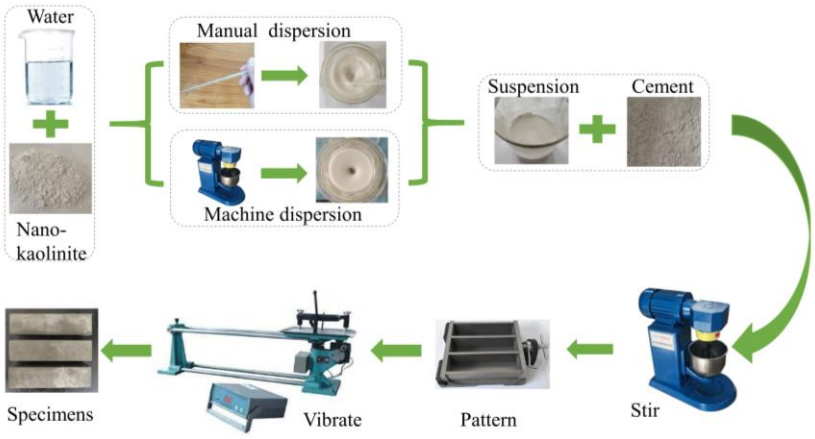

Figure 2. Preparation process.

2.3. Test Methods

2.3.1. Mechanical Properties Tests

After the test pieces were cured to the specified age under standard curing conditions, the DYE-300S automatic flexural and compressive machine was used to test the flexural and compressive strength of the cement-based materials, following the relevant provisions of the current Chinese standard test method for cement mortar strength (ISO method) (GB/T 17671-2021).

2.3.2. Scanning Electron Microscopy (SEM)

In this test, a SUPRA 55 SAPPHIRE was used to observe the internal microstructural changes of the specimen; in order to reduce the test error, the samples in the centre part of the crushed specimen were selected and made into thin slices, which were soaked in anhydrous ethanol to stop hydration. Then, the slices were dried in a vacuum at 50 °C for 48 h. The samples were firstly glued to the specimen with conductive adhesive and sprayed with gold so that the specimen had electrical conductivity, then it was turned on for observation.

2.3.3. Mercury Intrusion Porosimetry (MIP)

In this study, mercury intrusion porosimetry tests were performed on the pores of the cement paste specimens using a MicroActiveAutoPore V 9600. The pressure range was 0.10~60,000.00 psi, and the contact angle of the mercury with the pore surface was $\theta = 130^{\circ}$. When preparing mercury pressure specimens, samples were taken from the cement specimens that had been cured for 28 days. The specimens were cut into small pieces of approximately 3–5 mm using scissors, and each sample was taken for at least two tests. After sampling, the cement specimens were soaked in anhydrous ethanol for at least 24 h to terminate the hydration reaction. Before the mercury compression test, the specimens were taken out of the air to allow the ethanol to develop fully and then dried in a drying oven at 50 °C until a constant mass was reached, and the free water and ethanol were evaporated before the mercury intrusion porosimetry test was carried out.

2.3.4. Calculation of the Surface Fractal Dimension

The pores of cement-based materials are usually irregular and disorderly distributed; unlike the traditional assumption of smooth, straight, isometric, and regular, its pores, area, volume, etc, in all scales, show fractal characteristics.

The fractal dimensions of a cement-based material with porous properties can be analysed using the Zhang model [32]. Nano-kaolinite refinement of pores and pozzolanic reactivity can affect the surface shape of pores. Therefore, the Zhang model, which is suitable for analysing the effect of nano-kaolinite on the pore surface shape, was used in this study. In this model, the surface energy added by the mercury on the pore surface of

the cemented material is equal to the work done by the mercury injected in the mercury intrusion porosimetry test.

$$W_n = \sum_{i=1}^{n} \overline{P_i} \Delta V_i \tag{1}$$

$$Q'_n = \frac{V_n^{1/3}}{r_n} \tag{2}$$

where W_n and Q'_n are calculated from the mercury pressure data, n is the interval of the applied mercury pressure, $\overline{P_i}$ is the average pressure, ΔV_i is the volume of mercury feed for different pressure intervals, V_n is the total amount of mercury feed, and r_n is the diameter of the pore corresponding to the n th feed.

$$\ln(\frac{W_n}{r_n^2}) = D \ln Q'_n + \ln C \tag{3}$$

where D is the surface fractal dimension, and C is a constant. The slope of the linear fit using Equation (3) is the surface fractal dimension, D. The surface fractal dimension of the Zhang model is in the range of $2 < D < 3$; when the surface fractal dimension is close to 2, the pore surface is smooth, and when the surface fractal dimension is close to 3, the shape becomes more complex.

3. Results and Discussion

3.1. Mechanical Properties

In order to understand the impact of nano-kaolinite dispersion on the mechanical properties of cement specimens, the mechanical properties (i.e., flexural strength, compressive strength) of nano-kaolinite cement specimens were studied and analysed to obtain the law of the influence of nano-kaolinite on the mechanical properties of the cement-based materials.

3.1.1. Flexural Strength

The flexural strengths of the nano-kaolinite-modified cement specimens at different ages are shown in Table 6.

Table 6. Results of flexural strength tests.

Sample	Flexural Strength/MPa			
	3 Day	7 Day	14 Day	28 Day
NC0	4.56	6.01	7.07	7.45
NCH1	5.31	6.42	7.64	8.07
NCH2	5.42	6.51	8.24	8.96
NCH3	5.51	6.53	8.36	8.74
NCM1	5.49	6.52	7.90	8.45
NCM2	5.63	6.55	8.60	9.09
NCM3	5.79	6.66	8.89	9.40

The results show that the flexural strengths of the specimens with the added nano-kaolinite are all enhanced compared to the flexural strengths of the reference group. In the later stage, at 28 days, the flexural strengths of the specimens mixed with nano-kaolinite increased compared with those of the reference group. The increase was more significant than in the early stage, in which the flexural strength of the mechanically dispersed specimens reached up to 9.36 MPa. In comparison, the flexural strength of the cement specimens of the reference group was 7.45 MPa at this time. This indicates that incorporating a certain amount of nano-kaolinite can improve the flexural strength of cement specimens, and the increase in the age of curing increases the flexural strength more obviously. The main reason why nano-kaolinite can improve the flexural strength of cement is due to the small diameter

effect of its particles, which fill the pores in the cement and increase the compactness of the cement, and the fact that nano-kaolinite, which is capable of pozzolanic reactivity, produces additional C-S-H gels, which further increases the compactness of the cement, and thus improves its flexural strength.

In the early stage, the flexural strength of the specimen with nano-kaolinite was increased by 10.81% compared with that without nano-kaolinite at 7 days. At 28 days, the flexural strength of the specimen with nano-kaolinite was increased by 27.79%. With the increase in curing age, the nano-kaolinite promotes hydration, the hydration products accumulate, and the flexural strength is improved. However, the flexural strength of the mechanically dispersed specimens was generally higher than that of the manually dispersed specimens due to the agglomeration of the nano-kaolinite in the manually dispersed specimens, which prevented its filling effect and pozzolanic reactivity from taking place.

Comparing manually dispersed and mechanically dispersed specimens, it can be found that the early and late strengths of the mechanically dispersed specimens are higher than those of the manually dispersed specimens. This is because mechanical dispersion can effectively improve the dispersibility of nano-kaolinite, which gives full play to its filling effect, nucleation effect, and pozzolanic reactivity. It can better fill the pores, increase the C-S-H production, and improve the microstructure and porosity [33], thus improving the flexural properties of the cement.

3.1.2. Compressive Strength

The compressive strengths of the nano-kaolinite cement specimens at different ages are shown in Table 7.

Table 7. Results of compressive strength tests.

Sample	Compressive Strength/MPa			
	3 Day	7 Day	14 Day	28 Day
NC0	24.58	30.79	37.68	44.05
NCH1	26.78	32.69	39.21	45.03
NCH2	26.95	33.12	40.16	46.98
NCH3	27.65	33.66	39.87	45.54
NCM1	27.33	33.30	40.20	45.97
NCM2	27.03	33.74	41.56	48.34
NCM3	28.30	34.17	42.16	47.12

The results show that the compressive strength of the cement specimens increased with the increase in the dosage of nano-kaolinite. The compressive strength of the mechanically dispersed specimens reached a maximum of 28.30 MPa at the early age of 3 days, an increase of 15.13% compared to the reference group specimens. The maximum compressive strength of the mechanically dispersed specimens reached 48.34 MPa at 28 days of age, an increase of 9.74% compared to the reference group. This is due to the effect of the nano-kaolinite filling the small pores in the cement specimens and the pozzolanic reactivity of the nano-kaolinite to produce additional C-S-H gels, which increases the compactness of the cement and thus the compressive strength of the cement specimens. This is similar to known findings [11,33].

The compressive strength of mechanically dispersed specimens is better than that of manually dispersed specimens because mechanical dispersion breaks down agglomerated nano-kaolinite to give good dispersion. In contrast, agglomeration of nano-kaolinite occurs in the manually dispersed specimens, resulting in a poorer improvement. At 28 days of age, the compressive strength did not improve significantly when the nano-kaolinite dosing exceeded 1%. This was mainly due to the increase in nano-kaolinite dosing, which made it difficult to disperse the nano-kaolinite and caused agglomeration of nano-kaolinite particles, which prevented the filling effect and pozzolanic reactivity of the nano-kaolinite.

3.2. Microstructure of Cement Paste

Figure 3 shows the microstructure of the nano-kaolinite cement samples with different dispersion modes. As can be seen from the figure, in the cement specimens without nano-kaolinite, the microstructure is looser, and there are more interconnected pores, needle and rod ettringite (AFt) crystals, and square plate $Ca(OH)_2$(CH) crystals observed in the microstructure, and needles or fibres dominate the C-S-H gels. The C-S-H gels are mainly agglomerated in the cement specimens with manually dispersed nano-kaolinite. The number of pores increased due to the agglomeration of nano-kaolinite. In the cement specimens with mechanically dispersed nano-kaolinite, the number of pores and connected pores decreased, and the C-S-H gels were mainly in granular form and tightly packed together, which tightly wrapped the AFt crystals and C-H crystals. In addition, the number of AFt crystals increased in the C-S-H gel. A large amount of C-S-H gel fills the pore structure, forming a dense and uniform microstructure [34]. This indicates that the mechanically dispersed nano-kaolinite has good dispersibility, making the cement specimens denser.

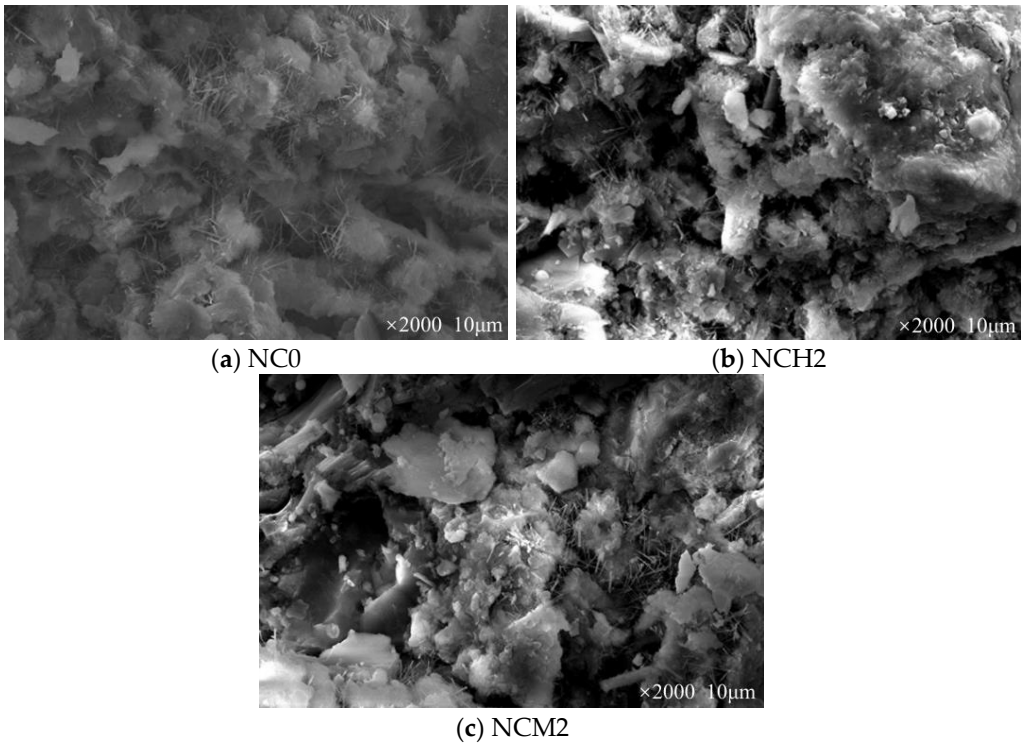

(**a**) NC0 (**b**) NCH2

(**c**) NCM2

Figure 3. Microstructure of cement specimens with different dispersion methods.

3.3. Pore Structure Characteristics

In order to analyse the pore distribution of the cement samples in-depth, the changes in the characteristic parameters, such as porosity, average pore diameter, median pore diameter, most probable pore diameter, and pore diameter distribution of the nano-kaolinite cement specimens(age 28 days), with different dosing focused on the mixing method.

3.3.1. Most Probable Pore Diameter

The most probable pore diameter is the peak pore diameter on the differential curve of the pore diameter distribution. In other words, the pore diameter with the largest number of pores in the specimen [35]. The pore diameter distribution can be reflected, to some extent, by the maximum pore diameter; the smaller the maximum pore diameter, the smaller the corresponding average pore diameter, and the more pronounced the refinement of the pore structure. On the contrary, the larger the maximum pore diameter, the looser the pore structure. The differential curves of the cement specimens are shown in Figure 4, the most probable pore diameters are shown in Table 8.

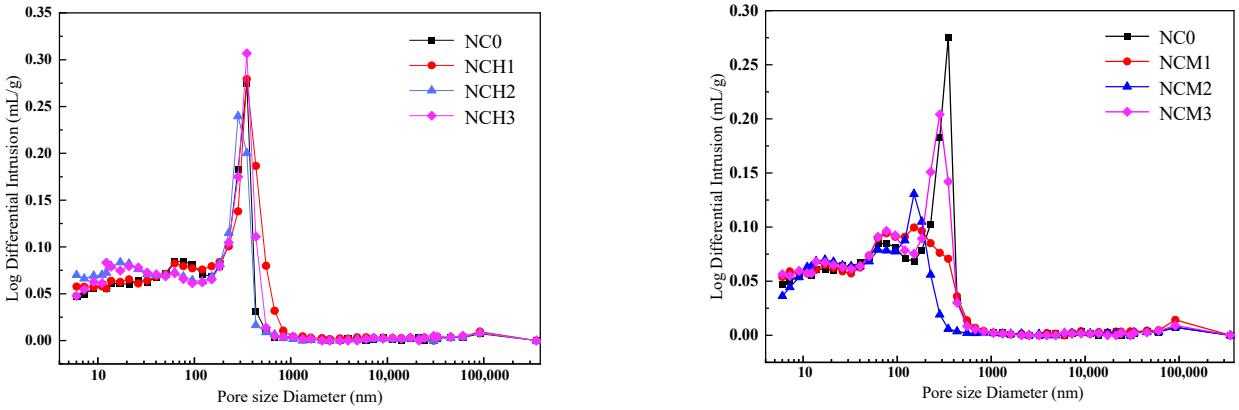

Figure 4. Differential curves of pore diameter distribution for two types of dispersed specimens.

Table 8. Most probable pore diameters.

Sample	NC0	NCH1	NCH2	NCH3	NCM1	NCM2	NCM3
Most probable pore diameter	349.92	349.81	284.09	350.11	151.04	151.01	283.97

It can be seen in Figure 4 that both dispersions have different degrees of improvement in the most probable pore diameter. After the nano-kaolinite is mixed in, the nano-kaolinite particles fill the pores in the cement, making the cement pore structure improve and refine. Whether by manual or mechanical dispersion, the improvement effect was more obvious when the nano kaolinite was mixed at 1%, and the porosity decreased by 18.81% and 56.84%, respectively; however, when the nano kaolinite was mixed at more than 1%, the improvement effect on the most probable pore diameter decreased with the increase. This is due to the agglomeration phenomenon caused by the excessive content of nano-kaolinite, which could not be evenly dispersed in the cement and had no obvious filling effect on the pore structure of the cement specimen, resulting in the weakening of the improvement effect of the nano-kaolinite on the most probable pore diameter. Meanwhile, the improvement effect of mechanical dispersion on the most probable pore diameter was better than that of manual dispersion. Figure 4 shows that the peak values and corresponding pore diameters of the mechanically dispersed nano-kaolinite specimens were reduced to different degrees, i.e., the most probable pore diameter was reduced significantly, by 56.83%, 56.84%, and 18.82%, respectively, compared with those of the benchmark specimens. It was concluded that agglomeration of manually dispersed nano-kaolinite occurs, and nano-kaolinite cannot be uniformly dispersed in the cement, resulting in an insignificant improvement effect. Compared with manual dispersion, mechanical dispersion can lead to better dispersion of nano-kaolinite. The nano-kaolinite particles significantly impact the refinement and filling of the pore structure, and the improvement of the pore structure is also greater.

3.3.2. Porosity, Average and Median Pore Diameter

It can be seen from Table 9 that the porosity of the mechanically dispersed nano-kaolinite specimens decreased to different degrees compared with the benchmark specimens. In particular, when the nano-kaolinite content was 1%, the porosity decreased more obviously, as high as 18.47%; when the nano-kaolinite content was 1.5%, the porosity increased, which may be due to the excessive nano-kaolinite content and the inability to disperse evenly. This shows that adding a certain amount of nano-kaolinite can improve the pore structure and make it denser. The table shows that the average and median pore diameters of the mechanically dispersed samples were reduced to different degrees, indicating that the nano-kaolinite was uniformly dispersed. The agglomerated kaolinite nanoparticles were dispersed during the mechanical mixing process, thus filling the pores and acting as nucleation sites for the C-S-H gels to accelerate the hydration of the cement, significantly

reducing the mean and median pore diameter. Manually dispersed nano-kaolinite does not disperse uniformly, so the improvement in mean and median pore diameter is not significant. Adding 1% nano-kaolinite with mechanical dispersion showed the most significant decrease in the mean and median pore diameter compared to the reference group, by 20.64% and 43.26%, respectively. These results indicate that nano-kaolinite can refine the pore structure and increase the density of cement, and the best effect was achieved at 1% of nano-kaolinite, but the effect on the improvement of average pore diameter and median pore diameter gradually decreased with the increase in dosing. The dispersion method influences the dispersibility of the nano-kaolinite, and mechanical dispersion results in better dispersibility.

Table 9. Pore space of cement specimens with different dispersion methods.

Sample	NC0	NCH1	NCH2	NCH3	NCM1	NCM2	NCM3
Porosity	28.42	32.11	29.43	30.60	26.47	23.17	28.78
Average pore diameter	40.7	44.4	34.2	39.7	35.7	32.3	38.3
Median pore diameter	121.6	179.5	98.8	138.6	92.9	69.0	108.0

3.3.3. Pore Diameter Distribution and Pore Surface Area

The pore diameter distribution of the cement specimens is shown in Figure 5. The effect of porosity on strength varies in each pore class. In this study, the pores of the cement materials were classified into four types of pores, harmless pores (less than 20 nm), less harmful pores (20–100 nm), harmful pores (100–200 nm), and more harmful pores (greater than 200 nm) [36]. After the addition of the nano-kaolinite, the proportion of harmful pores and more harmful pores decreased to different degrees, while the proportion of harmless pores and less harmful pores increased. That is, the pore size distribution developed into smaller pores. It can be concluded that the pore structure becomes dense after doping with nano-kaolinite. This indicates that nano-kaolinite can refine the pores and make the pore diameter develop towards a smaller pore diameter. Both manual dispersion and mechanical dispersion showed the highest percentage reduction of harmful pores and more harmful pores at 1% nano-kaolinite doping, but the refining effect gradually weakened when the nano-kaolinite doping exceeded 1%. This indicates that the agglomeration of nano-kaolinite occurs when the nano-kaolinite is dosed too much, which leads to a less obvious refinement effect and affects the pore diameter distribution of the cement specimens to some extent. By comparing the two dispersion methods, it can be seen that mechanical dispersion has a slightly better refinement effect on pore diameter distribution than manual dispersion, which also indicates that mechanical dispersion better disperses the nano-kaolinite, so it can play its role of filling pores and achieve the effect of refining pore diameter.

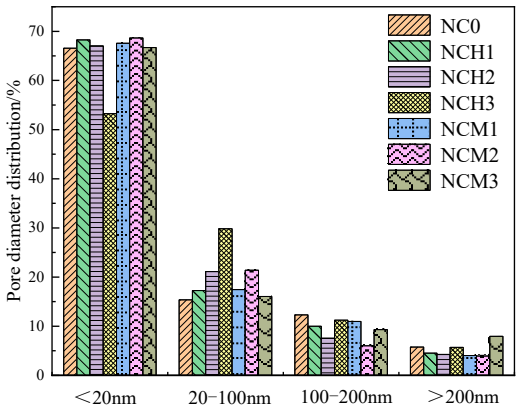

Figure 5. Pore diameter distribution.

The pore surface area of the cement specimens is shown in Figure 6, which shows that the pore surface area of the mechanically dispersed specimens is lower than that of the manually dispersed specimens. This indicates that the mechanical dispersion achieves better dispersibility, so the nano-kaolinite is better dispersed and decreases the pore surface area. When the dosage was increased to 1.5%, the improvement effect was reduced. This is because the amount of nano-kaolinite is too much to cause uniform dispersion.

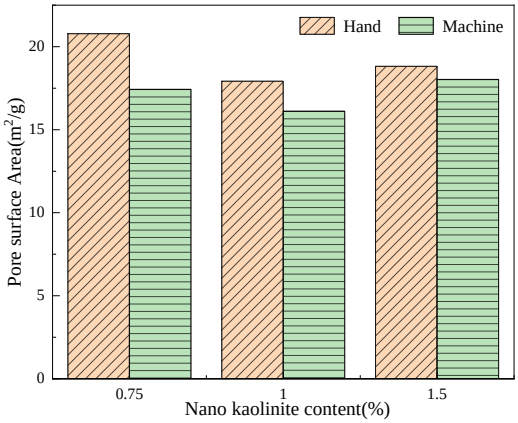

Figure 6. Pore surface area.

3.4. Relationship between Fractal Dimension and Pore Structure Characteristics

3.4.1. Surface Fractal Dimension

Considering the complex, irregular, and disordered internal structure of cement-based materials, using fractal theory to investigate the pore diameter distribution characteristics of nano-kaolinite cement-based materials can help reveal their microstructural characteristics. Therefore, based on the test results of the MIP method, the fractal characteristics of the pore structure of nano-kaolinite cement-based materials were further investigated.

The surface fractal dimension was calculated by linearly fitting the MIP data of the nano-kaolinite specimens with different mixing methods, as shown in Table 8. The calculated fractal dimensions were all in the range of 2.90–2.95, consistent with the definition of the fractal dimension of the pore surface area in the range of $2 < D < 3$ in the Zhang model. This indicates that the nano-kaolinite cement-based material has a distinct fractal character.

The complexity was classified according to the absolute values of the surface fractal dimension, as shown in Table 10. Among them, the mechanically dispersed 1% nano-kaolinite specimens had the smallest pore fractal dimension and were therefore considered to have the lowest complexity among all the samples. The surface fractal dimension of the remaining specimens had different degrees of change from the reference group specimens, so their complexity also had different degrees of change. This indicates that incorporating nano-kaolinite changes the complexity of the pore structure. The surface fractal dimension of manual dispersion showed a similar trend to that of mechanical dispersion, which indicates that the dispersion method affects the dispersion of nano-kaolinite and impacts the pore structure, thus changing the surface fractal dimension. It is seen that the fractal dimension of the mechanical mixing is lower than that of the manual mixing at different nano-kaolinite dosages, indicating that mechanical dispersion can better reduce the complexity and irregularity of the pore structure. This is consistent with the results of the pore diameter characterisation. The fractal dimension tends to increase when the nano-kaolinite dosing exceeds 1%, which means that the effect of nano-kaolinite on the complexity of the pore structure decreases as the dosing increases because the nano-kaolinite cannot be dispersed uniformly and is prone to agglomeration.

Table 10. Fractal dimension of the pore surface area for each specimen.

Sample	NC0	NCH1	NCH2	NCH3	NCM1	NCM2	NCM3
Surface fractal dimension	2.9374	2.9423	2.9291	2.9271	2.9177	2.9069	2.9216
Correlation coefficient	0.9942	0.9964	0.9952	0.9936	0.9932	0.9913	0.9896

3.4.2. Surface Fractal Dimension and Mechanical Properties

The relationship between the surface fractal dimension and the flexural and compressive strength of the nano-kaolinite cement specimens is shown in Figures 7 and 8. This indicates that the surface fractal dimension can characterise the flexural and compressive strength of the cement specimens, to some extent, and that incorporating nano-kaolinite increases the cement specimens' flexural and compressive strength and improves the cement specimens' internal complexity. The fractal dimension can reflect the relationship between the microscopic pore structure characteristics and mechanical properties of cement specimens.

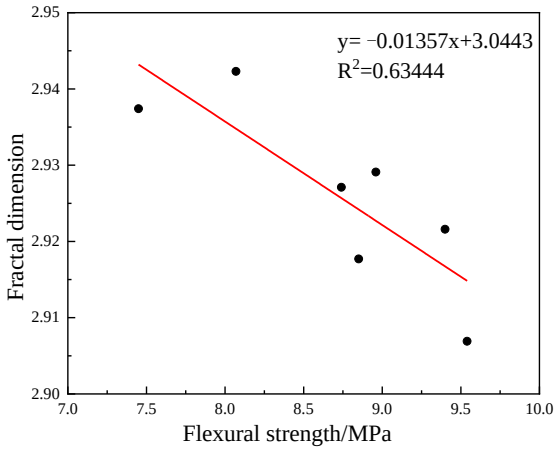

Figure 7. Fractal dimension and flexural strength.

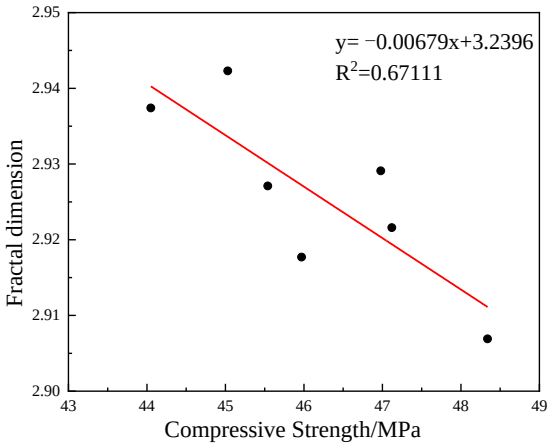

Figure 8. Fractal dimension and compressive strength.

3.4.3. Surface Fractal Dimension and Most Probable Pore Diameter

Figure 9 shows the surface fractal dimension as a function of the most probable pore diameter. It can be seen that the surface fractal dimension increases with the increase in the most probable pore diameter. This shows that the surface fractal dimension correlates well with the most probable pore diameter, consistent with Han et al. [37]. The smaller the surface fractal dimension, the smaller the corresponding most probable pore diameter, and

the smaller the corresponding average pore diameter, the more obvious the refinement of the pore structure and the lower the complexity of the pores. This means that nano-kaolinite reduces the complexity of the pores while reducing the most probable pore diameter.

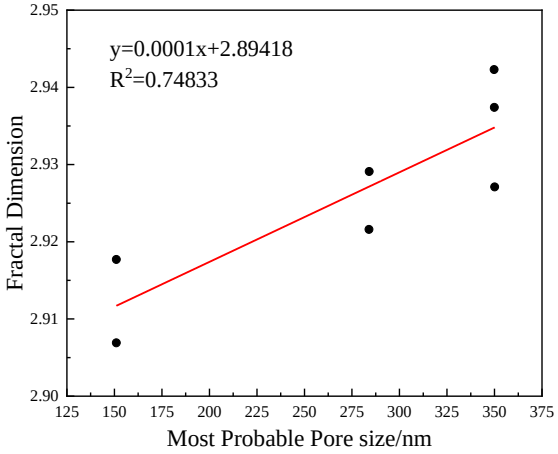

Figure 9. Fractal dimension and most probable pore diameter.

3.4.4. Surface Fractal Dimension and Porosity, Mean Pore Diameter, and Median Pore Diameter

Figure 10 shows the relationship between the surface fractal dimension and the porosity. It can be seen that as the porosity increases, the surface fractal dimension also increases. The porosity characterises the amount of pore space within the cement-based material. The surface fractal dimension of the specimens doped with nano-kaolinite decreases as the porosity decreases, implying that the nano-kaolinite reduces the complexity of the pores while reducing the porosity.

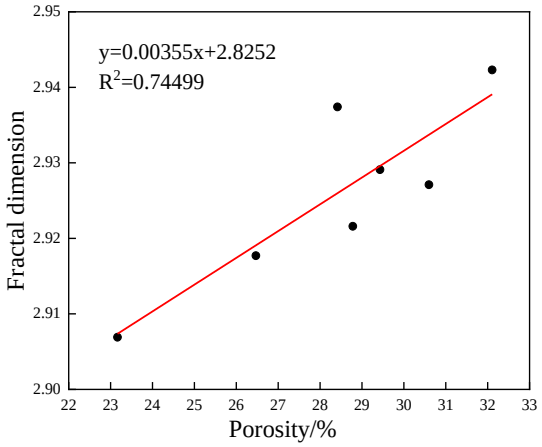

Figure 10. Fractal dimension and the porosity.

The average and median pore diameters are parameters that characterise the average pore diameter and reflect the pore diameter distribution. The larger the pores in the pore structure, the larger the average and median pore diameter. Conversely, the smaller the pores, the smaller the average and median pore diameter. Figures 11 and 12 show the relationship between the fractal dimension and the mean and median pore diameter, respectively. It can be seen that the fractal dimension correlates well with the average and median pore diameter. As the average pore diameter and median pore diameter of nano-kaolinite cement-based materials increase, the fractal dimension of the pore surface area also tends to increase accordingly. This indicates that the spatial distribution of the pore structure tends to be more complex as the number of macropores increases.

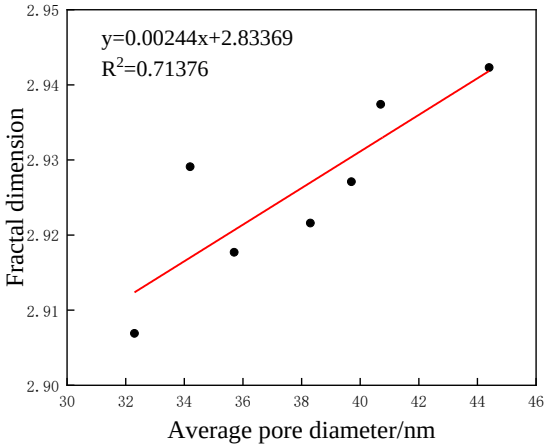

Figure 11. Fractal dimension and average pore diameter.

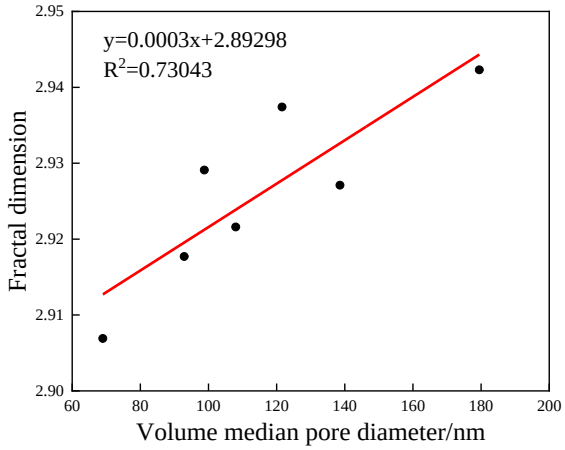

Figure 12. Fractal dimension and median pore diameter.

3.4.5. Surface Fractal Dimension and Pore Surface Area

For the same porosity, the larger the pore surface area of the nano-kaolinite cement sample, the greater the roughness of the pore surface, i.e., the pore surface area of the pore structure reflects, to some extent, the complexity of the pore diameter. Figure 13 shows the relationship between the pore surface area and the surface fractal dimension. It can be seen that the pore surface area is positively correlated with the surface fractal dimension and has a good correlation.

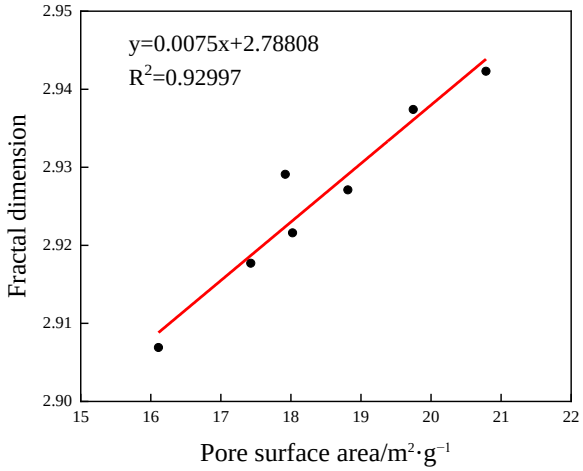

Figure 13. Fractal dimension and pore surface area.

4. Conclusions

(1) The dispersibility of nano-clay is influenced by the dispersion method. The appropriate amount of nano-kaolinite particles mixed into the cement-based material can improve the pore structure, refine the pores, and improve the durability of the cement-based material. The most significant improvement in the pore structure of cement is achieved when the nano-kaolinite is mixed at 1%. Mechanical dispersion can improve the dispersibility of nano-kaolinite so that the nano-kaolinite particles fill the larger pores in the cement more effectively and improve its pore structure. As the admixture of nano-kaolinite increases, agglomeration occurs. It cannot be completely dispersed in the cement material, and the improvement effect on the pore structure of the cement is reduced.

(2) The fractal characteristics of the nano-kaolinite cement-based materials in this paper are obvious, and the calculated surface fractal dimension is consistent with the existing models, which are all in the range of 2.90–2.95. The fractal dimension can clearly describe the internal pore characteristics of the pores, and the surface fractal dimension has a good correlation with the conventional parameters of the pores. Well-dispersed nano-kaolinite can refine the pore structure and reduce the fractal dimension. Compared with other pore structure characterization parameters, the surface fractal dimension can be considered a comprehensive parameter to characterise the pore morphology and space distribution, which can accurately reflect the pore structure characteristics.

(3) There is an excellent linear relationship between the integral shape dimension of the pore surface and flexural and compressive strength. As the fractal dimension increases, the internal complexity of the cement specimens increases, the pores become disorganized, and the mechanical properties are reduced. As a parameter that can characterise the complexity of the pore structure, the fractal dimension can reflect the relationship between the microscopic pore structure characteristics and the compressive strength of cement specimens.

(4) The surface fractal dimension reveals that the pore size distribution of cement-based materials varies on a microscopic scale. It provides a new method for studying pore structure. When combined with pore structure characteristic parameters, it can well reflect the pore structure characteristics and complexity of nano-kaolinite cement materials.

Author Contributions: Writing—original draft, funding acquisition, H.W.; writing—review and editing, C.C.; resources, formal analysis investigation, W.Z. (Wei Zhang); resources, formal analysis investigation, R.W.; methodology, W.Z. (Wengang Zhang). All authors have read and agreed to the published version of the manuscript.

Funding: This research was funded by the Fundamental Research Funds for the Central Universities, grant number 31920200033, the Fundamental Research Funds for the Central Universities, grant number 31920220126, and the Intelligent monitoring of slope of Dingxi-Lintao Expressway and civil experimental of BIM application samples, grant number Z22030, for which the authors are very grateful.

Data Availability Statement: Not applicable.

Acknowledgments: The authors gratefully acknowledge the support received from the Fundamental Research Funds for the Central Universities.

Conflicts of Interest: The authors declare no conflict of interest.

References

1. Wang, C.; Zhang, P.; Guo, J.; Wang, J.; Zhang, T. Durability and microstructure of cementitious composites under the complex environment: Synergistic effects of nano-SiO_2 and polyvinyl alcohol fiber. *Constr. Build. Mater.* **2023**, *400*, 132621. [CrossRef]
2. Yu, F.; Guo, J.; Liu, J.; Cai, H.; Huang, Y. A review of the pore structure of pervious concrete: Analyzing method, characterization parameters and the effect on performance. *Constr. Build. Mater.* **2023**, *365*, 129971. [CrossRef]
3. Kawashima, S.; Wang, K.; Ferron, R.D.; Kim, J.H.; Tregger, N.; Shah, S. A review of the effect of nano-clays on the fresh and hardened properties of cement-based materials. *Cem. Concr. Res.* **2021**, *147*, 106502. [CrossRef]
4. Tejas, S.; Pasla, D. Assessment of mechanical and durability properties of composite cement-based recycled aggregate concrete. *Constr. Build. Mater.* **2023**, *387*, 131620. [CrossRef]

5. Alharbi, Y.R.; Abadel, A.A.; Mayhoub, O.A.; Mohamed, K. Effect of using available metakaoline and nano materials on the behavior of reactive powder concrete. *Constr. Build. Mater.* **2021**, *269*, 121344. [CrossRef]
6. Chen, Y.; Li, X.; Du, H. A review of high temperature properties of cement based composites: Effects of nano materials. *Mater. Today. Commun.* **2023**, *35*, 105954. [CrossRef]
7. Li, Q.; Fan, Y.; Shah, S.P. Effect of nano-metakaolin on establishment of internal structure of fly ash cement paste. *J. Build. Eng.* **2023**, *77*, 107484. [CrossRef]
8. Douba, A.E.; Hou, P.; Kawashima, S. Hydration and mechanical properties of high content nano-coated cements with nano-silica, clay and calcium carbonate. *Cem. Concr. Res.* **2023**, *168*, 107132. [CrossRef]
9. Mohamed, H.; Ivon, M.H.; Shereen, A.; Noha, S.I. Improvement of cement pastes composite properties containing clay nanoparticles. *Ceram. Silik.* **2020**, *64*, 398–406.
10. Mohamed, H.; Ibrahim, N.S. Hydration, microstructure and phase composition of composite cements containing nano-clay. *Constr. Build. Mater.* **2016**, *112*, 19–27.
11. Mohamed, H.; Hamdy, A.A.; Fuad, A.A. Positive impact performance of hybrid effect of nano-clay and silica nano-particles on composite cements. *Constr. Build. Mater.* **2018**, *190*, 508–516.
12. Shoukry, H.; Kotkata, M.F.; Abo-EL-Enein, S.A.; Morsy, M.S. Flexural strength and physical properties of fiber reinforced nanometakaolin cementitious surface compound. *Constr. Build. Mater.* **2013**, *43*, 453–460. [CrossRef]
13. Farzadnia, N.; Ali, A.A.A.; Demirboga, R.; Anwar, M.P. Effect of halloysitenanoclay on mechanical properties, thermal behavior and microstructure of cement mortars. *Cem. Concr. Res.* **2013**, *48*, 97–104. [CrossRef]
14. Langaroudi, M.A.M.; Mohammadi, Y. Effect of nano-clay on workability, mechanical, and durability properties of self-consolidating concrete containing mineral admixtures. *Constr. Build. Mater.* **2018**, *191*, 619–634. [CrossRef]
15. Hong, Z.; Zuo, J.; Zhang, Z.; Liu, C.; Liu, L.; Liu, H. Effects of nano-clay on the mechanical and microstructural properties of cement-based grouting material in sodium chloride solution. *Constr. Build. Mater.* **2020**, *245*, 118420. [CrossRef]
16. Morsy, M.S.; Shoukry, H.; Mokhtar, M.M.; El-Khodary, S.A. Facile production of nano-scale metakaolin: An investigation into its effect on compressive strength, pore structure and microstructural characteristics of mortar. *Constr. Build. Mater.* **2018**, *172*, 243–250. [CrossRef]
17. Shebl, S.S.; Seddeq, H.S.; Aglan, H.A. Effect of micro-silica loading on the mechanical and acoustic properties of cement pastes. *Constr. Build. Mater.* **2011**, *25*, 3903–3908. [CrossRef]
18. Kong, D.; Huang, S.; Corr, D.; Yang, Y.; Shah, S.P. Whether do nano-particles act as nucleation sites for C-S-H gel growth during cement hydration? *Cem. Concr. Compos.* **2018**, *87*, 98–109. [CrossRef]
19. Zhang, S.; Fan, Y.; Jia, Z.; Ren, J. Effect of nano-kaolinite clay on rebar corrosion and bond behavior between rebar and concrete. *J. Mater. Civil. Eng.* **2021**, *33*, 402–416. [CrossRef]
20. Khaloo, A.; Mobini, M.H.; Hosseini, P. Influence of different types of nano-SiO_2 particles on properties of high-performance concrete. *Constr. Build. Mater.* **2016**, *113*, 188–201. [CrossRef]
21. Hamed, N.; El-Feky, M.S.; Kohail, M. Effect of nano-clay de-agglomeration on mechanical propertiesof concrete. *Constr. Build. Mater.* **2019**, *205*, 245–256. [CrossRef]
22. Qin, Q.; Meng, Q.; Yi, P.; Wu, K.; Wang, C. Investigation on the rheology, self-shrinkage, pore structure, and fractal dimension of coral powder-cement slurry. *J. Build. Eng.* **2023**, *77*, 107517. [CrossRef]
23. Lü, Q.; Qiu, Q.; Zheng, J.; Wang, J.; Zeng, Q. Fractal dimension of concrete incorporating silica fume and its correlations to pore structure, strength and permeability. *Constr. Build. Mater.* **2019**, *228*, 116986. [CrossRef]
24. Pia, G.; Sanna, U. An intermingled fractal units model and method to predict permeability in porous rock. *Int. J. Eng. Sci.* **2014**, *75*, 31–39. [CrossRef]
25. Zarnaghi, V.N.; Fouroghi-Asl, A.; Nourani, V.; Ma, H. On the pore structures of lightweight self-compacting concrete containing silica fume. *Constr. Build. Mater.* **2018**, *193*, 557–564. [CrossRef]
26. Choi, Y.C.; Park, B. Effects of high-temperature exposure on fractal dimension of fly-ash-based geopolymer composites. *J. Mater. Res. Technol.* **2020**, *9*, 7655–7668. [CrossRef]
27. Yang, J.; Huang, J.; He, X.; Su, Y.; Tan, H.; Chen, W.; Wang, X.; Strnadel, B. Segmented fractal pore structure covering nano-and micro-ranges in cementing composites produced with GGBS. *Constr. Build. Mater.* **2019**, *225*, 1170–1182. [CrossRef]
28. Jin, S.; Zheng, G.; Yu, J. A micro freeze-thaw damage model of concrete with fractal dimension. *Constr. Build. Mater.* **2020**, *257*, 119434. [CrossRef]
29. Wang, L.; Jin, M.; Wu, Y.; Zhou, Y.; Tang, S. Hydration, shrinkage, pore structure and fractal dimension of silica fume modified low heat Portland cement-based materials. *Constr. Build. Mater.* **2021**, *272*, 121952. [CrossRef]
30. Wang, J.; Wang, X.; Ding, S.; Ashour, A.; Yu, F.; Lv, X.; Han, B. Micro-nano scale pore structure and fractal dimension of ultra-high performance cementitious composites modified with nanofillers. *Cem. Concr. Compos.* **2023**, *141*, 105129. [CrossRef]
31. Pantić, V.; Šupić, S.; Vučinić-Vasić, M.; Nemeš, T.; Malešev, M.; Lukić, I.; Radonjanin, V. Effects of Grinding Methods and Water-to-Binder Ratio on the Properties of Cement Mortars Blended with Biomass Ash and Ceramic Powder. *Materials* **2023**, *16*, 2443. [CrossRef] [PubMed]
32. Zhang, B.; Li, S. Determination of the surface fractal dimension for porous media by mercury porosimetry. *Ind. Eng. Chem. Res.* **1995**, *34*, 1383–1386. [CrossRef]

33. Rıza, P.; Abdul, W.Q.; Fatma, K. Influence of singular and binary nanomaterials on the physical, mechanical and durability properties of mortars subjected to elevated temperatures and freeze–thaw cycles. *Constr. Build. Mater.* **2021**, *295*, 123608.
34. Fan, Y.; Zhang, S.; Wang, Q.; Surendra, P.S. The effects of nano-calcined kaolinite clay on cement mortar exposed to acid deposits. *Constr. Build. Mater.* **2016**, *102*, 486–495. [CrossRef]
35. Khatib, J.M.; Mangat, P.S. Influence of superplasticizer and curing on porosity and pore structure of cement paste. *Cem. Concr. Compos.* **1999**, *21*, 431–437. [CrossRef]
36. Li, G.; Zhou, J.; Yue, J.; Gao, X.; Wang, K. Effects of nano-SiO_2 and secondary water curing on the carbonation and chloride resistance of autoclaved concrete. *Constr. Build. Mater.* **2020**, *235*, 117465. [CrossRef]
37. Han, X.; Wang, B.; Feng, J. Relationship between fractal feature and compressive strength of concrete based on MIP. *Constr. Build. Mater.* **2022**, *322*, 126504. [CrossRef]